Viability, Adhesion and Differentiated Phenotype of Articular Chondrocytes on Degradable Polymers and Electro-Spun Structures Thereof

Tobias Schneider,[1,4] *Benjamin Kohl,*[1] *Tilman Sauter,*[2,3] *Tino Becker,*[2] *Karl Kratz,*[2,3] *Michael Schossig,*[2] *Bernhard Hiebl,*[2] *Friedrich Jung,*[2,3] *Andreas Lendlein,*[2,3] *Wolfgang Ertel,*[1] *Gundula Schulze-Tanzil*[*1]*

Summary: Degradable polymers are essential to enable biomaterial-based regenerative therapies, particularly, in articular cartilage defect healing, which remains a major clinical challenge. The aim of this study was to investigate the effect of two degradable polymers (as a film or scaffold) on primary articular chondrocytes vitality, adherence, differentiated phenotype and morphology. Films and electro-spun scaffolds were prepared from degradable poly(ether)ester urethane (PDC), which was synthesized via co-condensation of poly(*p*-dioxanone)diol and poly(ε-caprolactone)-diol with an aliphatic diisocyanate and poly(*p*-dioxanone) (PPDO). The thermal and mechanical properties and the surface roughness of the films and scaffolds were examined by differential scanning calorimetry, dynamic mechanical thermal analysis, tensile tests and optical profilometry. Primary porcine articular chondrocytes were seeded on the polymers and analysed for viability, ultrastructure (scanning electron microscopy) and immunolabelled for type II collagen. All films and scaffolds exhibited a low endotoxin load < 0.06 EU/ml and only moderate cytotoxic effects when tested with L929 cells. The results of the seeding experiments revealed that survival and adhesion of chondrocytes depended strongly on seeding density. Vital chondrocytes could be detected on both PPDO and PDC films and scaffolds. They produced the cartilage-specific protein type II collagen indicating differentiated functions. However, they exhibited a mixed morphology on the films and a more flattened cell shape on the scaffolds. The cell/biomaterial interaction in the PPDO scaffolds or films was more intense compared to that in PDC topologies.

The polymer topology influences chondrocytes phenotype, whereby the scaffolds permitted a more continuous cell growth compared with the films.

Keywords: chondrocytes; degradable polymer; differentiation; electro-spinning; multiblock copolymer

[1] Department for Orthopaedic, Trauma and Reconstructive Surgery, Campus Benjamin Franklin, Charité-Universitätsmedizin Berlin, Garystrasse 5, 14195 Berlin, Germany
E-mail: gundula.schulze-tanzil@charite.de
[2] Center for Biomaterial Development, Institute of Polymer Research, Helmholtz-Zentrum Geesthacht, 14513 Teltow, Germany
[3] Berlin-Brandenburg Center for Regenerative Therapies, 13353 Berlin, Germany
[4] University of Applied Science, 48149 Muenster, Germany

Introduction

In view of the poor intrinsic regeneration capability, articular cartilage injury remains an intriguing clinical problem. Therefore, biomaterial-based tissue engineering approaches which can induce endogeneous regeneration of critical sized defects are intensively studied.[1,2] Matrix assisted autologous chondrocyte implantation (MACI) is a commonly used technique for coverage of articular

cartilage defects.[2] For MACI, autologous chondrocytes were isolated, expanded *in vitro* and implanted into the articular cartilage defect in combination with a supporting scaffold. However, the available synthetic polymer scaffolds e.g. polyglycolide (PGA) but also biopolymers such as collagen or hyaluronic acid scaffolds have a rather rapid degradation rate. PGA degrades between 6–12 weeks *in vivo*.[3,4] Rapid mass and volume loss[5] can be associated with a local pH shift caused by temporarily high concentrations of degradation products. This acidic micromilieu can exhibit detrimental effects on the cells growing in the scaffold, induce some tissue inflammation and lead to a rapid loss of biomechanical stability. Hence, the implantation of autologous chondrocytes seeded on a biocompatible polymer with a controllable degradation behavior might be a promising approach to improve cartilage repair in future.[5] Biocompatibility is the absolute precondition to apply a biomaterial in medicine. In general biomaterials should exhibit no toxic effects and in case of articular cartilage regeneration the differentiated phenotype of the chondrocytes should not be influenced. 2D or 3D culture conditions can strongly affect the differentiation state of connective tissue cells such as chondrocytes.[6–8] Chondrocytes dedifferentiate when cultured on 2D surfaces such as tissue culture plastic. Their dedifferentiation comes along with rapid proliferation and is characterized by morphological alterations towards a flattened fibroblast-like phenotype, a severe decrease in the synthesis of cartilage-specific extracellular matrix proteins such as type II collagen and aggrecan as well as by a shift in the expression profile of multiple other ECM and cell surface proteins e.g. up-regulation of non-specific ECM proteins such as type I collagen and fibronectin.[8]

In the present study the influence of 2D and 3D topologies of a degradable poly-(ether)esterurethane consisting of poly(*p*-dioxanone) (PPDO) and poly(ε-caprolactone) (PCL) segments named PDC and pure PPDO on chondrocyte viability, adherence, growth and morphology was investigated. PDC was selected as candidate material, which shows linear mass loss in hydrolytic and enzymatic *in-vitro* degradation experiments and where the degradation rate can be controlled by changing the chemical composition (ratio of PPDO to PCL) of the polymer as well as the surface to volume ratio of the resultant scaffold.[9–12] It belongs to the class of multifunctional degradable materials, which are capable to exhibit a thermally-induced shape-memory effect[13,14] and therefore offer novel approaches to deliver bulky scaffolds in a condensed manner via minimally invasive surgery into the body.[15,16]

Methods

Polymers, Film and Scaffold Preparation

PDC was synthesized via co-condensation of identical weight contents of poly(ε-caprolactone)diol with a number-average molecular weight of $M_n = 2000$ g/mol and poly(p-dioxanone)diol $(M_n = 5300$ g/mol) using an hexamethylene diisocyanate according to the method recently described by Lendlein et al.[9,11] Poly(*p*-dioxanone)-diol as telechelic precursor was prepared by ring-opening polymerization of *p*-dioxanone with ethylene glycol as initiator. The resulting PDC exhibited a number-average molecular weight of $M_n = 75000$ g/mol and a polydispersity of PD = 12.3, which was determined by gel permeation chromatography (GPC). GPC measurements were conducted at ambient temperature on a multidetector GPC-system consisting of two 300 mm x 8.0 mm linear M columns (Polymer Standard Service, Mainz, Germany), an isocratic pump 2080 and an automatic injector AS 2050 (both Jasco, Groß-Umstadt, Germany), a RI detector Shodex RI-101 (Showa Denko Europe, Munich, Germany), and a differential viscometer/light scattering dual detector T60A (Viscotek Europe, Crowthorne, UK) using chloroform as eluent with a flow rate of 1.0 mL/min, and 0.2 wt-% toluene as internal standard.

PPDO (Resomer X®, Boehringer Ingelheim Pharma GmbH & Co., KG, Ingelheim, Germany) with an inherent viscosity of 1.5–2.2 dL/g determined in 0.1 wt-% in 1,1,1,3,3,3 hexafluoro-2-propanol (HFP) at 30 °C was used as received. 2D films were prepared from the melt by compression moulding of PDC and PPDO, while electro-spinning of scaffolds was conducted from HFP solution at ambient temperature according to the procedure described previously.[9] Briefly described, PPDO was processed into a non-woven scaffold with an electric field strength of 0.8 kV/cm, while the gap size was kept at 35 cm. For PDC an electric field strength of 0.7 kV/cm was applied at a gap size of 25 cm. Both polymers were electro-spun at a concentration of 11% (w/v) and a slowly rotating strip electrode was used for collecting the fibers.

Thermal and Mechanical Characterization

Differential scanning calorimetry (DSC) experiments were performed on a Netzsch DSC 204 Phoenix (Netzsch, Selb, Germany). All experiments were conducted in the temperature range from −100 to 150 °C with a constant heating and cooling rate of 10 K/min and with a waiting period of 2 minutes at the maximum and minimum temperature. Melting temperatures (T_m) were determined from the second heating run.

Dynamic mechanical thermal analysis (DMTA) at varied temperature was conducted on an Eplexor® 25 N (Gabo, Ahlden, Germany) equipped with a 25 N load cell. For the films test specimens of the type DIN EN ISO 1BB were used, for the scaffolds test specimens were cut into rectangular stripes with the dimensions $40 \times 10 \times 0.1$ mm^3. The heating rate was 2 K/min from −100 to 150 °C, and the applied oscillation frequency was 10 Hz. The glass transition temperature (T_g) was determined from the peak of the tan δ-temperature curve.

The mechanical properties of the electro-spun scaffolds and films were assessed by tensile tests (Z 2.5, Fa. Zwick, Ulm, Germany), which were conducted at ambient temperature using the same test specimen as for the DMTA measurements. Five consecutive measurements were performed for each material and structure. For determination of the Young's modulus (E) of the porous scaffolds an effective thickness d_{eff} was applied and calculated according to $d_{eff} = m_s/(w_s \cdot l_s \cdot \rho_p)$, where m_s, w_s and l_s are the mass, width and length of the test specimen and ρ_p is the density of the polymer.

Characterization of Surface Roughness of 2D Polymer Films

Surface profiles and roughness (R_q) of sterilized 2D films were investigated with an optical profilometer type MicoProf 200 (Fries Research & Technology GmbH; Hamburg, Germany) equipped with a CWL 300 chromatic white-light sensor. Scanning was repeated five times with a scanning area of 50×50 μm^2.

Scanning Electron Microscopy Analysis (SEM)

The electro-spun scaffolds were examined by SEM at different magnifications according to their morphology for determination of the fiber diameter. Pore sizes were determined using SEM images at 500x magnification by measuring the diameter of a virtual sphere in between embracing fibers, while only fibers of the in-focus plane were utilized for calculation. Pores and in-focus fibers were distinguished by a introducing a grey scale threshold. For both materials 3 samples were examined at 3 different sections. Each section covered an area of 50×50 μm^2, contained a minimum number of 10 pores with a pore size of at least 5 μm^2 and was analyzed using ImageJ software.[17]

To assess chondrocytes ultrastructure on the scaffolds and films SEM was performed after 36 and 72 hours culturing on the polymers. Samples were rinsed three times in 0.1 M cacodylate buffer (pH 7.2) before and after fixation for 2 hours in 4% (v/v) glutaraldehyde diluted in 0.1 M cacodylate at 4 °C in the dark. Finally, the samples were dehydrated in an ascending alcohol series at 4 °C and dried using hexamethyl-

disilazine for 3×10 minutes. Samples were anchored on a sample holder and supplied with a conductive interlayer. They were sputtered using platin/palladium (80:20) under vacuum (Polaron SC7640, Quorum Technologies, UK). SEM pictures were taken at 300–20.000x magnification and 1–3 kV using an Everhard-Thornley detector (Gemini Supra 40 VP, Zeiss, Jena, Germany).

Sterilization of the Samples

Scaffolds and films were sterilized using ethylene oxide. After preconditioning for 12 hours at 35–45 °C and 50–80% relative humidity, the samples were sterilized under the same conditions for 3 hours with 600 mg/l ethylene oxide and subsequently left for 3 days at 35–45 °C to induce desorption. Finally the samples were subjected to a nitrogen gas atmosphere at 50 °C for 48 hours under vacuum to remove all gas residues.

Investigation of Endotoxin Load and Cytotoxicity Testing

Prior to chondrocyte exposure the endotoxin content of the sample extracts was analyzed based on the endotoxin induced activation of a proenzyme in the lysate of *Limulus Amebocytes*. The resulting enzyme releases *p*-nitroaniline from a synthetic substrate, which can be photometrically detected and the concentration correlates linearly with the endotoxin content (QCL-10001 *Limulus Amebocyte* Lysate assay, Lonza).

The cytotoxicity tests in direct contact were performed in accordance to the supplier's instructions and in conformity with EN DIN ISO standard 10993-5. Disc-shaped polymer films (diameter: 14.0 mm, thickness: 0.3 mm) and electro-spun scaffolds fixed in 13 mm MINUSHEET® (MINUCELLS and MINUTISSUE Vertriebs GmbH, Bad Abbach, Germany) were seeded with L929 cells (ATCC, 6×10^4 cells/cm^2). After an incubation time period of 48 hours at 37 °C in a humidified atmosphere with 5% CO$_2$ the mitochondrial activity of the cells was measured using tetrazolium compound, which was mainly reduced by mitochondrial dehydrogenases to a coloured formazan product absorbed at 490 nm (MTS assay, Promega, Germany). In addition, the integrity of the cell plasma membrane was tested by measuring the activity of the cytoplasmatic enzyme lactate dehydrogenase, which was released by damaged cells in the cell culture supernatant (LDH-assay, Roche, Germany). The morphology of the cells was evaluated according to the USP 23-NF18 (US Pharmacopeial Convention) using a transmitted light microscope (phase contrast mode, Zeiss, Germany).

Chondrocytes Isolation

Porcine cartilage was harvested from the knee joint (cartilage from the femoral grove, condyles and retropatellar cartilage were pooled) of pigs (3–6 month old hybrid pigs [n = 10]). Connective tissue remnants from the joint capsules and bone were carefully removed. Porcine cartilage samples were subsequently minced into 1 mm slices and enzymatically digested with 0.4% pronase (7 U/mg, Roche, Basel, Switzerland) diluted in Ham's F-12/Dulbecco's modified Eagle's (DMEM) medium 1:1 [Biochrom AG, Berlin, Germany] for 1 hour at 37 °C and subsequently digested with 0.2% (w/v) collagenase (≥ 0.1 U/mg, SERVA Electrophoresis GmbH, Heidelberg, Germany) diluted in growth medium for 16 hours at 37 °C. Isolated chondrocytes were resuspended in growth medium (Ham's F-12/DMEM 1:1 containing 10% (v/v) fetal calf serum (FCS) [Biochrom AG], 25 µg/mL ascorbic acid [Sigma-Aldrich], 50 IU/mL streptomycin, 50 IU/mL penicillin, 0.5 µg/mL partricin, essential amino acids, 2 mM L-glutamine [all: Biochrom AG]) and seeded at 2.8×10^4 cells/cm^2 in culture flasks.

Chondrocytes Seeding onto Scaffolds

Primary porcine articular chondrocytes of the monolayer passages 1-3 were used for the seeding experiments. PDC and PPDO scaffolds as well as the films were placed in the wells of a 6 well plate. Scaffolds and

films equilibrated in chondrocyte growth medium containing 10% (v/v) FCS for at least two days. 2×10^5 chondrocytes in 50–70 µL growth medium were directly pipetted onto the scaffolds or films and let to adhere for 30 minutes at 37 °C in the incubator. Subsequently, 2 mL culture medium was added to each well. Chondrocytes were cultivated on the scaffold or films for 3–5 days.

Vitality Testing

Chondrocytes cultured on the polymers were analysed for viability. After washing with PBS, the chondrocytes polymer constructs were incubated in fluorescein diacetate (FDA) (3 µg/mL dissolved in acetone [stock solution], Sigma-Aldrich and further diluted 1:1000 in PBS [working solution]) for 15 min at 37 °C, rinsed three times with PBS before being counter-stained with ethidium bromide solution (1 µL dissolved in 1 mL PBS) for 1 minute in the dark at room temperature. The green or red fluorescence was visualized using fluorescence microscopy (Axioskop 40, Zeiss, Jena, Germany) and photos were taken using a color view II camera (Olympus, Europa Holding, Hamburg, Germany).

Type II, Type I Collagen and Fibronectin Immunolabelling

Constructs were fixed in 4% (v/v) paraformaldehyde for 15 minutes. Samples were rinsed in Tris buffered saline (TBS: 0.05 M Tris, 0.015 M NaCl, pH 7.6) before being blocked with protease-free donkey serum (5% (v/v) diluted in TBS) for 30 minutes at room temperature (RT). Subsequently, cells were rinsed and incubated with the polyclonal rabbit anti-type II or type I collagen antibody [27.5 µg/mL, both Acris Antibodies, Herford, Germany] and mouse-anti-fibronectin antibody (Dianova, Hamburg, Germany) in a humidifier chamber overnight at 4 °C. Constructs were subsequently washed with TBS before incubated with donkey-anti-rabbit-Alexa-Fluor®488 (10 mg/mL, Invitrogen, Carlsbad, USA) and donkey anti-mouse Cy3

(Invitrogen, CA, USA) secondary antibody for 30 minutes at RT. Negative controls included omitting the primary antibody during the staining procedure. Cell nuclei were counterstained using 4',6-diamidino-2-phenylindole (DAPI) (0.1 µg/mL, Roche, Basel, Switzerland). Labelled constructs were rinsed several times with TBS and examined using fluorescence microscopy (Axioskop 40, Carl Zeiss, Jena, Germany). Images were taken using a color view II camera (Olympus Soft Imaging Solution GmbH, Muenster, Germany).

Results and Discussion

All sterilized 2D test specimen showed an almost smooth surface with a root mean square roughness R_q around 60 nm ($R_{q,PDC} = 56 \pm 11$ nm; $R_{q,PDDO} = 57 \pm 8$ nm) nm) as measured by an optical profilometry. Electro-spun scaffolds with an average deposit thickness of 80 ± 20 µm and a fiber diameter of around 3 ± 1 µm showing a randomly fiber orientation could be achieved as visualized by the SEM images shown in Figure 1. The average pore diameter between the fibers was 6 ± 1 µm for PDC scaffolds and 7 ± 1 µm for PPDO scaffolds.

The obtained thermal and mechanical data for PDC and PPDO are summarized in Table 1. The PDC film and scaffold exhibited identical thermal properties with two distinct melting transitions (T_m) at 36 °C, which can be attributed to the crystalline PCL domains and at 90 °C related to the crystalline PPDO domains, indicating the phase segregated morphology of the multiblock copolymer. Furthermore, two distinct T_g could be observed in DSC as well as in DMTA measurements (determined from the maxima in the tan δ *versus* temperature curves). Hereby the lower T_g around -50 °C is related to the amorphous PCL domains, while the T_g around -10 °C is related to the amorphous PPDO domains. In contrast, for PPDO film and scaffold a T_g at 3 °C and a T_m at 107 °C were obtained. The obtained
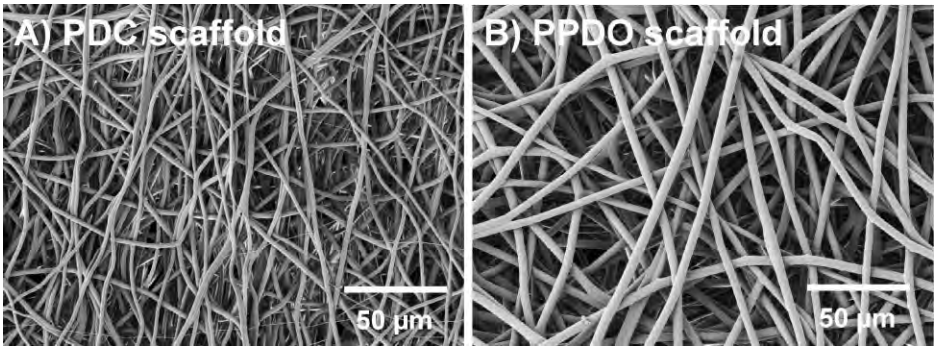
Figure 1.
SEM images of electro-spun PDC (A) and PPDO (B), Magnification: 500x: scale bar 50 μm.

thermomechanical properties of PDC were in good agreement with previously reported data.[9]

While for PPDO and PDC films a yield point could be observed in the stress-strain curves, no yield point was found for the corresponding scaffolds. The Youngs moduli determined for the scaffolds materials were substantially higher compared to that of the 2D films, while significant lower values for elongation of break ε_B were obtained for electro-spun scaffolds (see Table 1). The observed difference in mechanical properties of films and scaffolds can be attributed to a higher degree of orientation for the macromolecules in the electro-spun fiber based structures.

All films and scaffolds exhibited a low endotoxin load < 0.06 EU/mL and showed only moderate cytotoxic effects when tested with L929 cells. The success of the seeding experiments, depictured by chondrocytes adhesion and survival on the

polymers, strongly depended on seeding density. In response to low seeding cell densities (below 2×10^5 cells per scaffold) only a few adhering and surviving cells could be detected (not shown). Predominantly vital cells were found on both scaffolds of both polymers, PDC & PPDO and on the corresponding films at a seeding density of 2×10^5 cells per scaffold or film (Figure 2). However, on PDC but also PPDO the formation of cell clusters could often be observed.

In addition, the chondrocytes produced the cartilage specific type II collagen on all tested PDC and PPDO topologies indicating maintenance of differentiated functions (Figure 3). Type II collagen exhibited a pericellular distribution. Nonetheless, fibronectin synthesis was barely detectable at 72 hours culturing time (data not shown). Fibronectin expression is upregulated during chondrocytes dedifferentiation. Type I collagen, which is increasingly expressed in

Table 1.
Thermomechanical properties.

Sample	E^a [MPa]	$\varepsilon_B{}^a$ [%]	$T_{g,PCL}{}^b$ [°C]	$T_{g,PPDO}{}^b$ [°C]	$T_{m,PCL}{}^c$ [°C]	$T_{m,PPDO}{}^c$ [°C]
PDC film	22 ± 2	410 ± 30	−51 ± 1	−8 ± 1	36 ± 1	91 ± 1
PDC scaffold	51 ± 8	260 ± 25	−53 ± 1	−12 ± 1	36 ± 1	90 ± 1
PPDO film	230 ± 15	150 ± 30	–	5 ± 1	–	107 ± 1
PPDO scaffold	350 ± 30	130 ± 10	–	1 ± 1	–	107 ± 1

[a]Young's modulus (E) and elongation at break (ε) were obtained by tensile tests at room temperature.
[b]Glass transition temperature (T_g) was determined from tan δ vs. temperature curve in DMTA measurements.
[c]Melting transition temperature (T_m) was determined by DSC.
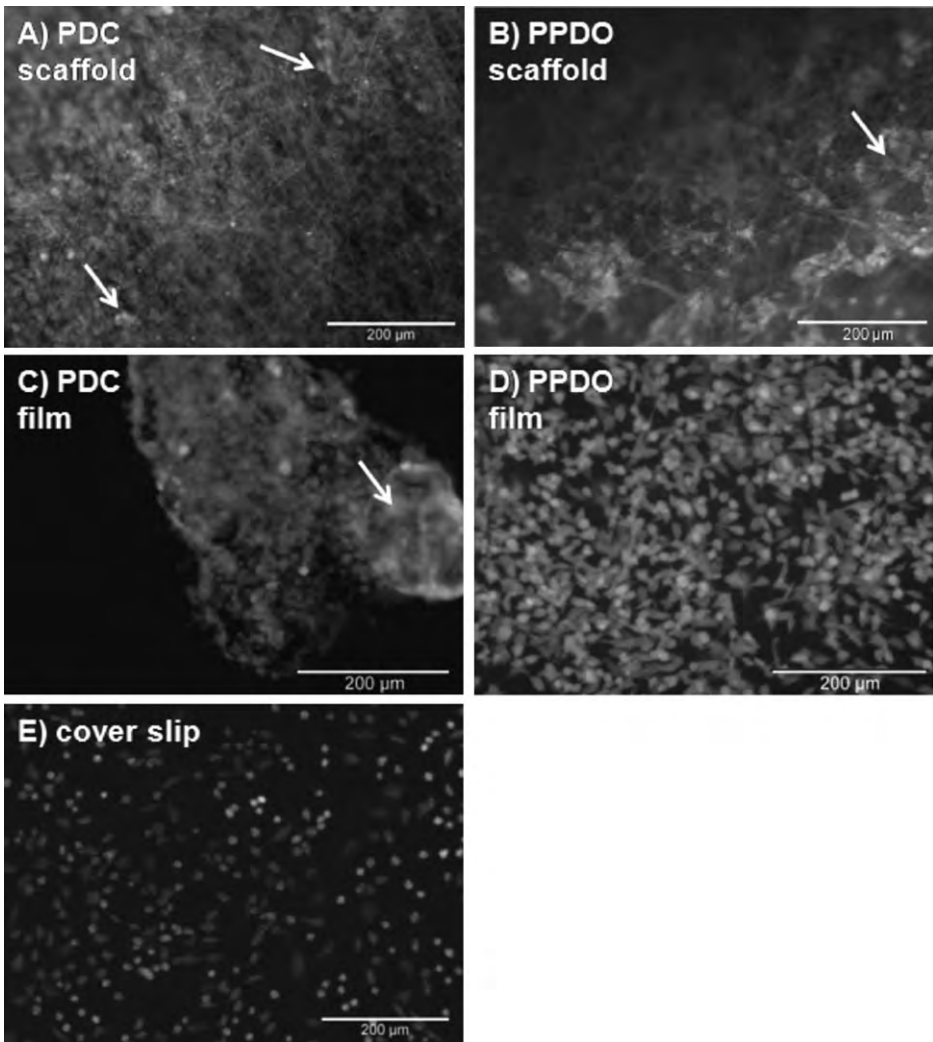
Figure 2.
Vitality test of articular chondrocytes seeded on PDC and PPDO polymer scaffolds, respective films and cover slips. Scaffolds and films were adapted in culture medium before seeded with chondrocytes and cultured for 5–6 days. Cell density: 2×10^5 cells per scaffold or film. Scale bars: 200 µm.

dedifferentiating chondrocytes is also detectable at a comparable immunoreactivity level (Figure 4). It seemed to be stronger expressed on glass cover slip cultures than by scaffold or film cultured chondrocytes.

The fiber diameter ($\sim 3\,\mu$m) of both polymer scaffolds was comparable. PDC scaffolds showed to a higher extend conglutinated fibers (Figure 5A, asterisks),

predominately at the fiber crossing points. This fact resulted in slightly lower pore sizes compared with PPDO. PDC scaffolds revealed also some variations in the fiber diameters within the same scaffold (Figure 1A and 5A). The PDC film exhibited a particular rough surface whereas that of the PPDO film was smooth (Figure 5C, D).

The SEM analysis revealed mostly flattened shaped chondrocytes with multiple
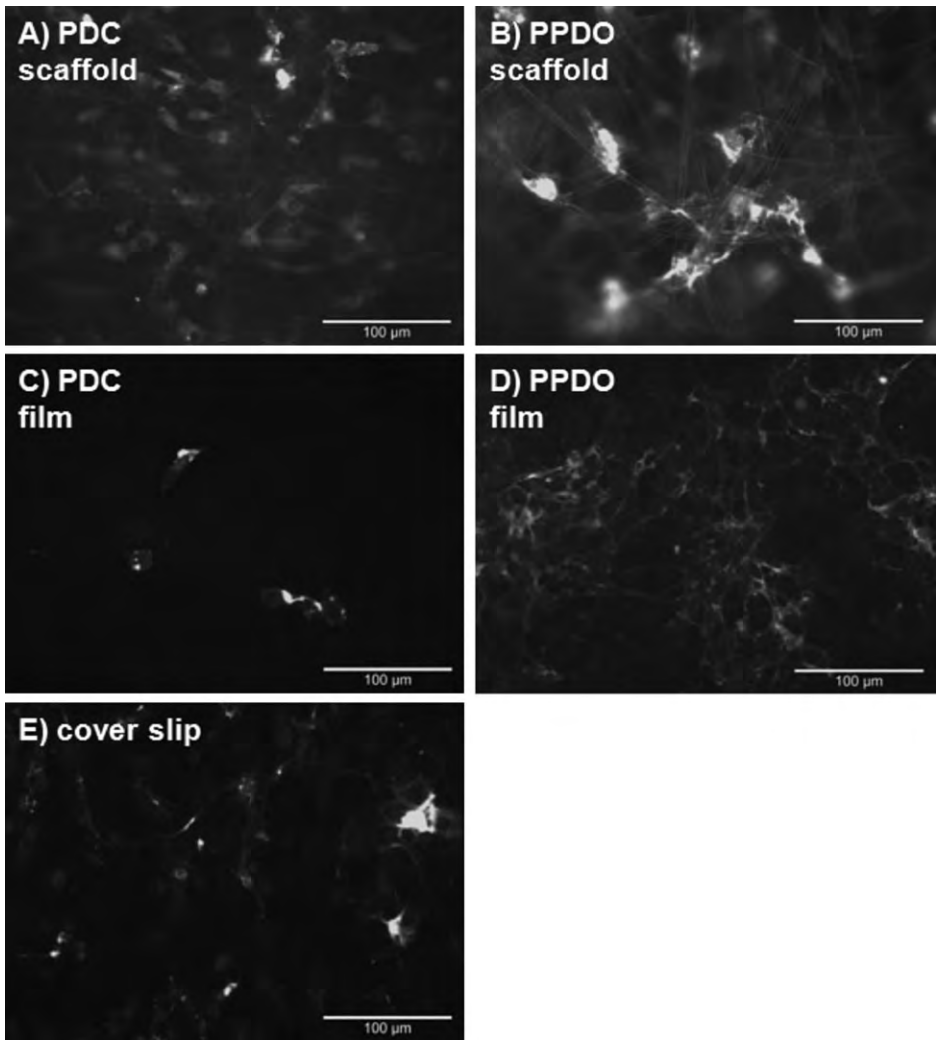
Figure 3.

Type II collagen expression of articular chondrocytes cultured on PDC and PPDO polymer scaffolds, respective films or cover slips. Scaffolds and films were pre-incubated in culture medium before seeded with chondrocytes for 5 days. Cell density: 2×10^5 cells per scaffold or film. Cell nuclei were counterstained using DAPI. Scale bars: 100 μm.

cellular extensions. Chondrocytes nestled in the surface layer of the scaffolds spanning their cytoplasmic extensions between several individual fibers. They barely immigrated into the interconnecting scaffolds pores, which appeared to be too small to let them pass. The chondrocytes were able to circum-grow the fibers of both polymers. They exhibited both filo- and lamellopodia to adhere at the fibers, whereby on PDC filopodia seem to predominate compared with lamellopodia (Figure 5A, B). On the films both, flattened cells and chondrocytes, rounding up could be detected (Figure 5C, D). However, chondrocytes contact to the fibers was more intense on the PPDO compared to the PDC film (Figure 5C, D). No signs of fiber degradation could be detected during the culture period. However, at 36 hours no major extracellular
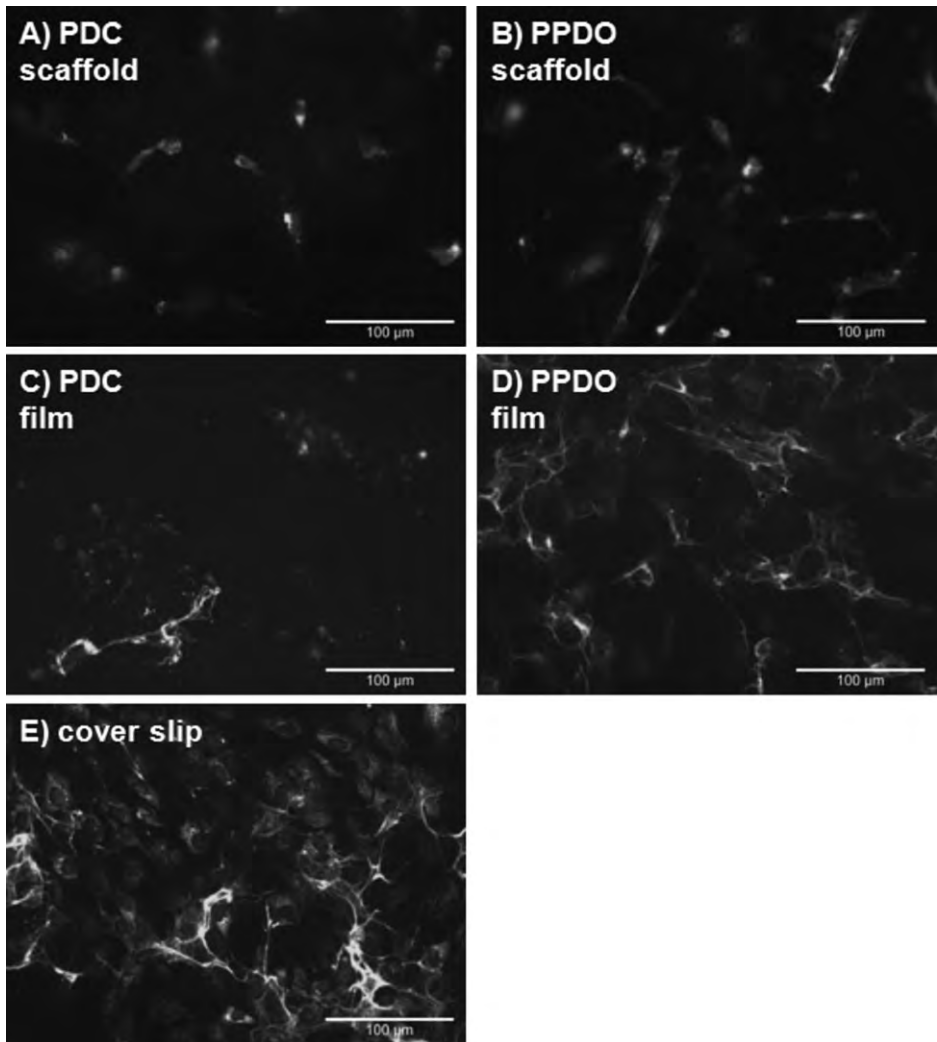
Figure 4.
Type I collagen expression of articular chondrocytes cultured on PDC and PPDO polymer scaffolds, respective films or cover slips. Scaffolds and films were pre-incubated in culture medium before seeded with chondrocytes for 5 days. Cell density: 2×10^5 cells per scaffold or film. Cell nuclei were counterstained using DAPI. Scale bars: 100 μm.

matrix or biofilm production by the chondrocytes was evident. Only some small, spider web-like fibers were discernible (Figure 5A, B, white arrows). In contrast, at 72 hours the deposition of a felt-like extracellular matrix consisting of many small and few thicker fibers could be observed on both, the PDC and PPDO scaffolds, accumulating between and under the cells. At this investigation time (Figure 6) the cellular surfaces revealed more microvilli- and knob-like processes compared with the 36 hours investigation time point (Figure 5).

Small microfibers should mimic the fiber network of natural cartilage matrix and provide multiple attachment points for 3D orientation of the chondrocytes. Controlled degrading materials, which do not result in a sudden release of potentially acidic degradation products from the bulk
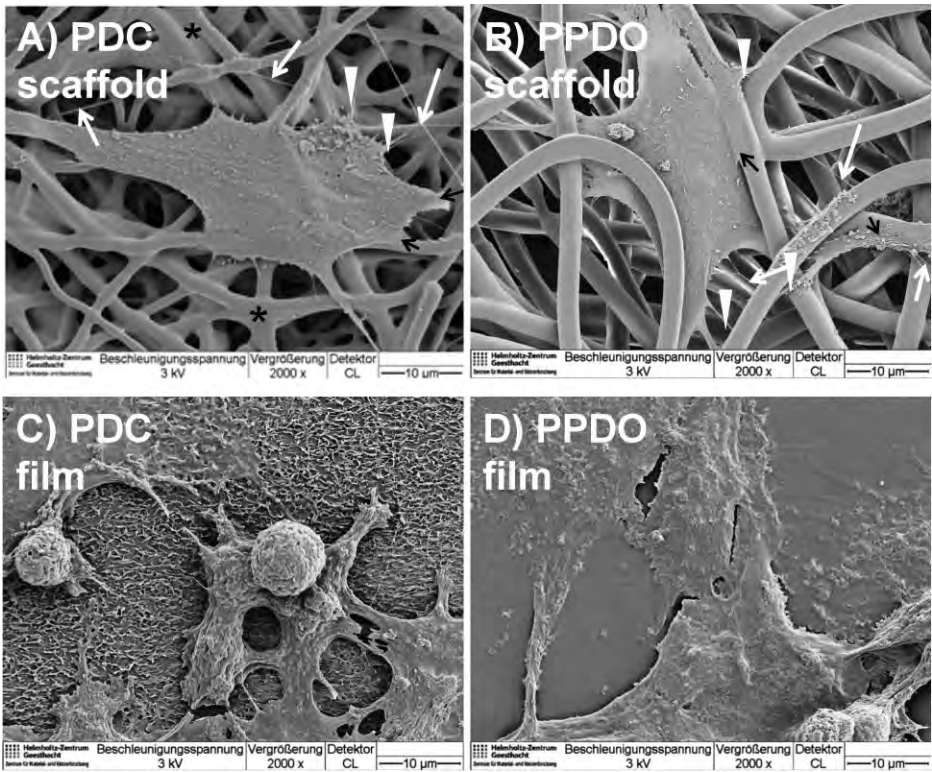
Figure 5.

SEM analysis of articular chondrocytes seeded on PDC and PPDO polymer scaffolds and films. Scaffolds (A, B) and films (C, D) were pre-incubated in culture medium. Chondrocytes were added and cultivated for 36 hours. Cell density: 2×10^5 cells per scaffold or film. Magnification: 2000x. Scale bars: 10 μm. *conglutinated scaffold fibers, white arrows: spider web-like ECM fibers, black arrows: lamellopodia, white arrowhead: filopodia.

material such as poly(*L*-lactide), could present improved biocompatibility and long lasting biomechanical strength and hence, an improvement in MACI. However, the aim of the study was not to provide a fully biomechanical competent scaffold able to sustain natural joint loading, but simply to test whether the material allows chondrocytes growth. The adaption of biomechanical properties should follow later. The tested PDC and PPDO topologies allow the growth of primary articular chondrocytes and maintenance of their differentiated functions as shown by type II collagen expression, which is the major cartilage-specific extracellular matrix protein. However, low seeding densities (lower than 2×10^5 cells per 14 mm diameter

scaffold) did not result in sufficient chondrocyte adhesion and growth on the polymers. Cells need cell-cell contacts and paracrine signaling for sufficient adherence and survival.

The extracellular matrix synthesis could also be shown on both polymers by SEM at longer culture time (72 hours). At this time chondrocytes cultured on the scaffold revealed features of synthetic and secretory activity such as areas of microvilli- and knob-like cell surface protrusions which have been reported by Schlegel et al., (2008) as a morphological correlate of chondrocytes differentiated funcions.[18] No fiber degradation and loss of stability could be detected morphologically during the experiments which comprised a pre-
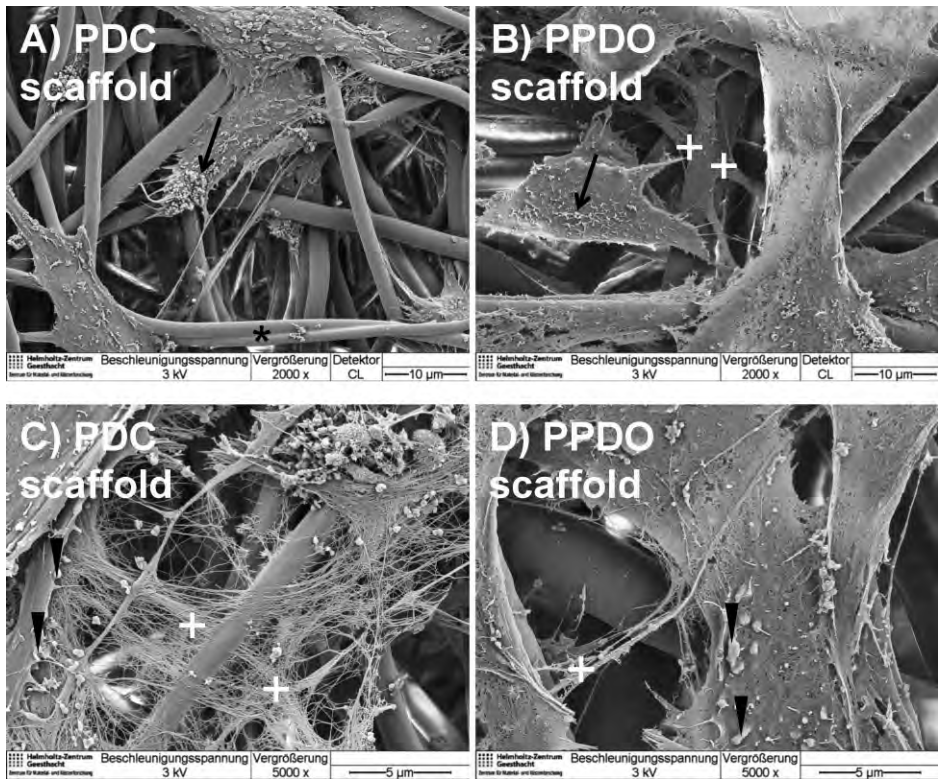
Figure 6.
SEM analysis of articular chondrocytes seeded on PDC and PPDO polymer scaffolds or respective films. Scaffolds and films were pre-incubated in culture medium. Chondrocytes were added and cultivated for 72 hours. Cell density: 2×10^5 cells per scaffold or film. Magnification: 2000x: scale bar 10 μm (A, B) and 5000x: scale bar 5 μm (C, D). Black arrows: mikrovilli-like cell protrusions, *conglutinated scaffold fibers, + felt-like ECM fibers, arrowhead: knob-like cell protrusions.

incubation phase of at least two days in culture medium containing 10% (v/v) FCS and a culture period of 5 days.

The topology (scaffold *versus* film) strongly influenced chondrocytes phenotype. Cells were not able to enter the pores of the scaffold which were smaller than the chondrocytes. Hence, the chondrocytes acquired mostly a flattened shape growing on the surface layers of the scaffold. A chondrocyte has a size of 16–60 μm depending on its time in culture. For this reason the scaffolds pore size should be adapted in future to allow chondrocyte immigration. In contrast, on the films most cells were flattened, but some cells exhibited a rounded shape. Cells, rounding up had an irregular and rather porous surface indicat-

ing that they might detach and probably undergo cell death. When seeded on the films, cells easily detached after longer cultivation times e.g. 72 hours as a typical feature of overconfluent 2D culture. This fact underlines the benefit of the scaffolds to allow a longer cultivation time of differentiated chondrocytes because of a high surface to volume ratio. Indeed, chondrocytes exhibited multiple lamello- and filopodia for fiber contact on the microfiber scaffolds.

Conclusion

The microfiber scaffold variants tested here present an interesting approach for

chondrocyte culture. Scaffolds are more preferable compared with the films for chondrocytes growth. PPDO allows the growth of a higher number of adherent cells than PDC. Further efforts should be undertaken to adapt and optimize scaffold topologies for chondrocytes: first of all, larger interconnecting pore sizes should be provided within the scaffolds to encourage chondrocytes migration into the scaffolds and 3D growth. Then, it is necessary to observe the chondrogenesis for a longer time period to assess ECM quality. Furthermore, several other parameters might be promising to improve chondrogenesis and scaffold handling such as a variation of the fibers diameters or a combination of larger and smaller diameter fibers within the same scaffold for its stabilization, or a modification of the surface structure of single fibers e.g. by supplying micropores to improve cell adherence. Last but not least, alignment of the fibers could provoke an orientation of the chondrocytes within the scaffold. The potential to influence cell orientation by the scaffold topology is of some concern since natural joint cartilage has a zonal organization which includes fiber and cell alignment.

[1] V. P. Shastri, A. Lendlein, *Advanced Materials* **2009**, *21*, 3231.

[2] E. B. Hunziker, *Osteoarthritis and Cartilage* **2002**, *10*, 432.

[3] A. Lohan, U. Marzahn, K. El Sayed, A. Haisch, B. Kohl, R. Müller, W. Ertel, G. Schulze-Tanzil, T. John, *Histochemistry and Cell Biology* **2011**, DOI 10.1007/s00418.

[4] C. Stoll, T. John, C. Conrad, A. Lohan, S. Hondke, W. Ertel, C. Kaps, M. Endres, M. Sittinger, J. Ringe, G. Schulze-Tanzil, *Biomaterials* **2011**, *32*, 4806.

[5] T. L. Spain, C. M. Agrawal, K. A. Athanasiou, *Tissue Engineering* **1998**, *4*, 343.

[6] P. D. Benya, J. D. Shaffer, *Cell* **1982**, *30*, 215.

[7] H. J. Hauselmann, K. Masuda, E. B. Hunziker, M. Neidhart, S. S. Mok, B. A. Michel, E. Thonar, *American Journal of Physiology-Cell Physiology* **1996**, *271*, C742.

[8] G. Schulze-Tanzil, *Annals of Anatomy* **2009**, *191*, 325.

[9] K. Kratz, R. Habermann, T. Becker, K. Richau, A. Lendlein, *International Journal of Artificial Organs* **2011**, *34*, 225.

[10] A. Kulkarni, J. Reiche, J. Hartmann, K. Kratz, A. Lendlein, *European Journal of Pharmaceutics and Biopharmaceutics* **2008**, *68*, 46.

[11] A. Lendlein, R. Langer, *Science* **2002**, *296*, 1673.

[12] D. Hofmann, M. Entrialgo-Castano, K. Kratz, A. Lendlein, *Advanced Materials* **2009**, *21*, 3237.

[13] M. Behl, U. Ridder, Y. Feng, S. Kelch, A. Lendlein, *Soft Matter* **2009**, *5*, 676.

[14] Y. K. Feng, M. Behl, S. Kelch, A. Lendlein, *Macromolecular Bioscience* **2009**, *9*, 45.

[15] A. Lendlein, M. Behl, B. Hiebl, C. Wischke, *Expert Review of Medical Devices* **2010**, *7*, 357.

[16] M. Sittinger, D. W. Hutmacher, M. V. Risbud, *Current Opinion in Biotechnology* **2004**, *15*, 411.

[17] T. Ferreira, W. Rasband, "ImageJ: Image Processing and Analysis in Java", US National Institute of Health, Bethesda, Maryland, USA, 2011, p. 2011/.

[18] W. Schlegel, S. Nurnberger, M. Hombauer, C. Albrecht, V. Vecsei, S. Marlovits, *Int J Mol Med* **2008**, *22*, 691.